RESEARCH ARTICLE
doi: 10.2306/scienceasia1513-1874.2026.071

ScienceAsia 52 (4): 2026: ID 2026071: **1–12**

Elamipretide coordinates OMA1/DELE1 signaling to modulate integrated stress response in cultured nucleus pulposus cells

Bo Lin, Shaoping Liu, Hongqiao Li, Yuanxue Tan*

Department of Orthopedics, Dangyang People's Hospital, Yichang 444100 China

*Corresponding author, e-mail: 15826700478@163.com

Received 28 Apr 2026, Accepted 16 Jul 2026
Available online 7 Aug 2026

ABSTRACT: Intervertebral disc degeneration (IDD) is a major cause of low back pain and disability. A central barrier is the unclear molecular link between mitochondrial dysfunction and the aberrant cellular stress responses that drive extracellular matrix breakdown, inflammation, and cell dysfunction in the nucleus pulposus (NP). Here, we identify the mitochondrial protease OMA1 as a previously unrecognized activator of the integrated stress response (ISR) in this context. Using LPS-induced inflammatory models, we show that OMA1 overactivation promotes the cleavage of its substrate DELE1, sustains eIF2α phosphorylation, and amplifies ATF4-dependent transcription, thereby exacerbating catabolic and pro-apoptotic programs. Conversely, the mitochondria-targeted peptide MTP-131 (or elamipretide) inactivates the OMA1/DELE1 pathway, suppresses ISR signaling, restores collagen and aggrecan synthesis, and reduces inflammatory cytokine release. These findings suggest the OMA1/DELE1 axis as a mechanistic hub that translates mitochondrial stress into disc pathology. It also reveals MTP-131 as a potential candidate for preserving mitochondrial homeostasis, offering a potential translational strategy for halting IDD progression.

KEYWORDS: mitochondrial function, integrated stress response, nucleus pulposus, elamipretide, inflammation

INTRODUCTION

Intervertebral disc degeneration (IDD) is the primary pathological basis of chronic low back pain, with core mechanisms including extracellular matrix (ECM) degradation, inflammatory responses, and cell apoptosis [1, 2]. Recent studies indicate that mitochondrial dysfunction plays a critical driving role in IDD. Nucleus pulposus (NP) cells, one of the predominant cell types in intervertebral discs, heavily rely on mitochondrial energy supply to maintain cellular homeostasis [3]. Mitochondrial dysfunction leads to insufficient adenosine triphosphate (ATP) synthesis, excessive accumulation of reactive oxygen species (ROS), and oxidative stress, thereby promoting apoptosis and accelerating ECM catabolism [4, 5]. Mitochondrial dysfunction may cause cytoplasmic mitochondrial DNA (mtDNA) accumulation, imbalance in mitochondrial biogenesis, and defective mitophagy, all of which exacerbate IDD progression [6, 7]. Dysregulation of mitochondrial quality control mechanisms is likely a key factor in IDD advancement, and therapeutic strategies targeting mitochondrial homeostasis repair could be beneficial for IDD treatment.

The integrated stress response (ISR) is an adaptive regulatory network activated by cells to counteract internal or external stressors, such as oxidative stress, nutrient deprivation, or protein misfolding [8]. Central to the ISR mechanism is the phosphorylation of eukaryotic translation initiation factor 2α (eIF2α) and the activation of downstream transcription factors like ATF4 and CHOP [9]. When mitochondrial function is impaired, the mitochondrial unfolded protein response is triggered to coordinate cellular adaptation to stress [10]. OMA1, a mitochondrial inner membrane protease, participates in mitochondrial unfolded protein response by cleaving mitochondrial proteins to adapt to mitochondrial depolarization or oxidative stress [11]. Under mitochondrial dysfunction, DELE1, a key substrate of OMA1, is cleaved by OMA1 to generate the truncated form (c-DELE1) [12]. Accumulation of c-DELE1 in the cytoplasm activates eIF2α, thereby modulating ISR. Targeting ISR holds significance for maintaining mitochondrial function and cellular homeostasis, though its therapeutic potential in IDD remains unclear.

Elamipretide (MTP-131), a synthetic peptide targeting the mitochondrial inner membrane, stabilizes mitochondrial membrane structure by selectively binding to cardiolipin and has been extensively studied in neurodegenerative and cardiovascular diseases [13, 14]. Research suggests that MTP-131 inhibits ROS production, preserves mitochondrial membrane potential, and protects cardiolipin from oxidative damage [15]. Additionally, MTP-131 enhances mitophagy to maintain mitochondrial quality control [15, 16]. However, the relationship between MTP-131 and ISR remains undefined. Given its close association with mitochondrial function, it is plausible that MTP-131 may influence cellular ISR by regulating mitochondrial proteins or enzymes. Furthermore, there are no reported studies on MTP-131 in IDD, leaving its mechanisms and therapeutic efficacy unexplored.

This study aims to investigate the pivotal role of OMA1 in ISR. Using LPS-induced inflammatory models of NP cells with OMA1 knockdown or overexpression, we examined the impact of OMA1 on inflammatory cytokine release and ECM metabolism. Our results

demonstrate that OMA1 promotes DELE1 cleavage, activating downstream ISR, a critical regulatory mechanism in NP cell degeneration. Further studies reveal that MTP-131 modulates OMA1 activation and DELE1 cleavage, thereby influencing ISR. These findings suggest that MTP-131 may serve as a promising therapeutic agent for mitigating NP cell inflammation and have potential for treating IDD.

MATERIALS AND METHODS

Isolation and culture of NP cells

All experiments have been approved by the Ethics Committee of Dangyang People's Hospital (No. 162).

Sprague-Dawley rats were provided by Hubei BIONT Biological Technology, China. Lumbar discs from 8-week-old Sprague-Dawley rats were surface-disinfected (75% ethanol), and nucleus pulposus (NP) tissues were excised. The tissue was washed three times with PBS and minced into small fragments. These fragments were digested with 0.25% type II collagenase (Sigma, Germany) for 6 h, then filtered through a 100 μm cell strainer to obtain a single-cell suspension. After centrifugation (1,200 rpm, 5 min), the cell pellet was resuspended in DMEM/F12 medium supplemented with 15% fetal bovine serum (Gibco, USA) and 1% penicillin/streptomycin. Cells were cultured in flasks at 37 °C with 5% CO_2, with medium changes every 3 days. Upon reaching 80% confluence, cells were passaged using 0.25% trypsin, and the second or longer passages were used for subsequent experiments.

Western blot analysis

After treatment, cells were washed three times with ice-cold PBS and lysed in RIPA buffer (containing 1% protease inhibitors) for 30 min. Lysates were centrifuged (12,000 rpm, 15 min, 4 °C), and total protein supernatants were quantified using a BCA assay kit (BioSharp, China). Equal protein amounts (30 μg) were separated via SDS-PAGE (4%–20% SurePAGE, GenScript, China) and transferred to a PVDF membrane (Millipore, USA) using wet transfer. Membranes were blocked for 15 min at room temperature with QuickBlock buffer (Beyotime, China) and incubated overnight at 4 °C with primary antibodies: anti-OMA1, anti-DELE1, anti-eIF2α, anti-p-eIF2α (1:2000); anti-ATF4 (1:1000); anti-Col2a1, anti-Acan, anti-Sox9 (1:1500). After washing with TBST, membranes were probed with HRP-conjugated secondary antibodies (rabbit or mouse, 1:10,000) for 1 h. All the primary and secondary antibodies were purchased from Proteintech company (Wuhan, China). Signals were visualized using ECL substrate (BioSharp) on a ChemiDoc system (Bio-Rad, USA), and band intensities were quantified by ImageJ with GAPDH as the loading control.

Flow cytometry for apoptosis

Treated cells were trypsinized, washed twice with PBS, and stained with 5 μl Annexin V-FITC and 10 μl PI using an Apoptosis Detection Kit (Beyotime) per the manufacturer's protocol. After 15 min of incubation in the dark, fluorescence was measured via flow cytometry (BD FACSCalibur, USA). FITC and ECD channels detected Annexin V^+/PI^- (early apoptosis) and Annexin V^+/PI^- (late apoptosis) populations, respectively. Data were analyzed using FlowJo software, with untreated cells as negative controls.

ELISA for cytokine quantification

Clarified supernatants (3,000 rpm × 10 min) were assayed for IL-1β/IL-6/TNF-α using commercial kits (BioSharp) according to protocols. Standards and samples were added to antibody-coated 96-well plates, incubated for 1 h at 37 °C, then reacted with biotinylated detection antibody and TMB substrate for 15 min. Absorbance (450 nm) was measured on a microplate reader (BioTek,USA), and cytokine concentrations were calculated from standard curves.

SiRNA synthesis and transfection

Gene-specific siRNAs and scrambled controls (si-scr) were designed and transfected using Lipo3000 (Invitrogen, USA). NP cells (50%–60% confluency in 6-well plates) were transfected with 50 nM siRNA in Opti-MEM for 6 h, followed by medium replacement. Knockdown efficiency was validated at 48 h post-transfection by quantitative polymerase chain reaction (PCR) or Western blot.

Plasmid construction and transfection

The CDS region of OMA1 was PCR-amplified, cloned into the pcDNA3.1(+) vector, and verified by sequencing. Recombinant plasmids (over-OMA1) and empty vectors (over-NC) were transfected into NP cells (2 μg/ml) using Lipo3000. After 48 h, transfection efficiency was assessed via fluorescence microscopy, quantitative PCR, or Western blot.

Co-immunoprecipitation (Co-IP)

For protein-protein interaction validation, cells were lysed in NP-40 buffer (with protease inhibitors). Cleared lysates (1 mg protein) were incubated with 5 μg anti-OMA1 overnight at 4 °C, followed by 4 h incubation with Protein A/G magnetic beads (MedChemExpress, China). Beads were washed three times, boiled in SDS-loading buffer, and subjected to Western blot (probed for DELE1). IgG served as a negative control.

Statistical analysis

All experiments were repeated at least 3 times ($n = 3$, biological replicates). Data are presented as

mean ± SD. Statistical analyses were performed using GraphPad Prism 8.0. Two-group comparisons were assessed with two-tailed unpaired *t*-tests, and multiple-group comparisons were evaluated by one-way or two-way analysis of variance (ANOVA) followed by Tukey's *post hoc* test. Significance was set at * $p < 0.05$, ** $p < 0.01$, or *** $p < 0.001$; "ns" denotes no significance ($p > 0.05$).

RESULTS

The ISR is activated in LPS-stimulated NP cells

LPS is a commonly used agent to induce cellular inflammation. We treated NP cells with different concentrations of LPS, and the results revealed that the expression levels of OMA1 and c-DELE1 increased with rising LPS concentrations (Fig. 1A). Phosphorylation of eIF2α is a critical step in initiating the ISR. LPS treatment dose-dependently enhanced the expression of phosphorylated eIF2α (p-eIF2α) and its downstream transcription factor ATF4 (Fig. 1B). Additionally, LPS significantly reduced ECM synthesis in NP cells, as evidenced by decreased levels of aggrecan, type II collagen, and the transcription factor Sox9 (Fig. 1C). LPS also markedly elevated the secretion of inflammatory cytokines such as IL-1β, IL-6, and TNF-α by NP cells (Fig. 1D). Furthermore, LPS induced apoptosis in NP cells, with the proportion of apoptotic cells progressively increasing with LPS concentration (Fig. 1E). Taken together, these results demonstrate that LPS activates the ISR and promotes ECM degradation, inflammatory activation, and apoptosis in NP cells.

OMA1 knockdown ameliorates the ISR and NP cell degeneration

To investigate the regulatory role of OMA1 in the ISR, we suppressed OMA1 gene expression using specific siRNA. The results showed that OMA1 expression was significantly reduced in the OMA1 knockdown group compared to the control group, accompanied by a decrease in c-DELE1 levels (Fig. 2A). Following OMA1 knockdown, the expression of ISR-associated molecules p-eIF2α and ATF4 was also markedly downregulated (Fig. 2B). Additionally, OMA1 knockdown ameliorated LPS-induced ECM degradation. Compared to the siRNA control group, protein expression levels of Acan, Col2a1, and Sox9 were significantly elevated in the OMA1 knockdown group (Fig. 2C). OMA1 suppression inhibited LPS-induced apoptosis in NP cells (Fig. 2D,E). Moreover, OMA1 knockdown significantly reduced the secretion of inflammatory cytokines IL-1β, IL-6, and TNF-α in NP cells compared to the siRNA control group (Fig. 2F). These findings collectively demonstrate that OMA1 knockdown alleviates ISR activation and NP cell inflammation and ECM degradation.

Overexpression of OMA1 aggravates the ISR and NP cell degeneration

To further validate the role of OMA1, we constructed an OMA1-overexpressed plasmid and transfected into NP cells. The results demonstrated that both OMA1 and c-DELE1 protein levels were significantly elevated in the OMA1 overexpression group compared to the control (Fig. 3A). OMA1 overexpression led to marked increases in ISR-associated molecules p-eIF2α and ATF4 (Fig. 3B). Furthermore, OMA1 overexpression exacerbated LPS-induced ECM degradation, with protein levels of Acan, Col2a1, and Sox9 significantly reduced compared to the overexpression control group (Fig. 3C). OMA1 overexpression promoted LPS-induced apoptosis in NP cells (Fig. 3D,E). Additionally, OMA1 overexpression significantly increased the secretion of IL-1β, IL-6, and TNF-α in NP cells relative to the overexpression control (Fig. 3F). These findings collectively indicate that OMA1 overexpression accelerates ISR activation and NP cell inflammation and ECM degradation.

OMA1 regulates the ISR via the eIF2α/ATF4 axis

To further elucidate the regulatory mechanism of OMA1 in ISR, we suppressed eIF2α expression using specific siRNA. Results revealed that OMA1 overexpression promoted DELE1 cleavage, whereas eIF2α knockdown did not significantly alter the c-DELE1 level (Fig. 4A). While OMA1 overexpression increased p-eIF2α and ATF4 expression, this effect was markedly attenuated following eIF2α knockdown (Fig. 4B). eIF2α suppression enhanced ECM anabolism in NP cells, with elevated protein levels of Acan, Col2a1, and Sox9 (Fig. 4C). Compared to the siRNA control group, eIF2α knockdown significantly reduced the secretion of IL-1β, IL-6, and TNF-α in NP cells (Fig. 4D). Moreover, eIF2α suppression inhibited OMA1 overexpression-induced apoptosis (Fig. 4E,F). These results demonstrate that OMA1 regulates ISR and NP cell degeneration through the eIF2α/ATF4 axis, driving ECM degradation, inflammatory activation, and apoptosis.

MTP-131 modulates the ISR in LPS-induced NP cells

MTP-131, known to stabilize mitochondrial membrane integrity, was investigated for its role in ISR regulation. Results showed that MTP-131 inhibited LPS-induced increases in OMA1 and c-DELE1 expression (Fig. 5A). MTP-131 treatment significantly suppressed eIF2α phosphorylation and reduced ATF4 expression (Fig. 5B). Additionally, MTP-131 enhanced ECM synthesis, increasing Acan, Col2a1, and Sox9 protein levels compared to the LPS-treated group (Fig. 5C). MTP-131 markedly attenuated the secretion of IL-1β, IL-6, and TNF-α in NP cells (Fig. 5D). Besides, the treatment of MTP-131 significantly suppressed LPS-

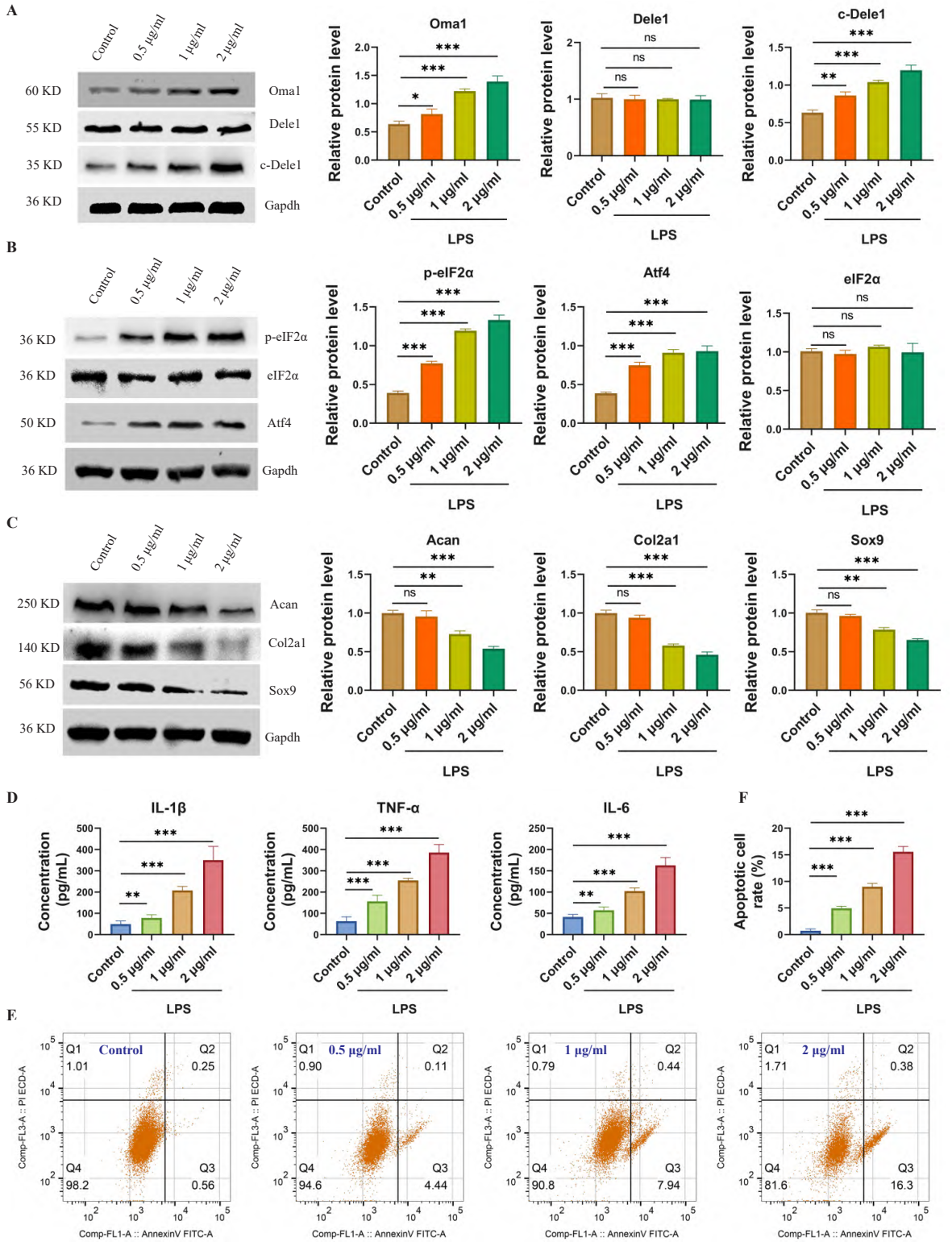

Fig. 1 LPS induces the ISR in NP cells. (A) Western blot and quantitative analysis of OMA1, DELE1, and c-DELE1 in NP cells treated with different doses of LPS (0.5, 1, 2 μg/ml). (B) Western blot and quantitative analysis of eIF2α, p-eIF2α, and ATF4 in NP cells treated with LPS. (C) Western blot and quantitative analysis of Acan, Col2a1, and Sox9 in NP cells treated with LPS. (D) ELISA results of secreted IL-1β, TNF-α, and IL-6 in NP cells treated with LPS. (E) Flow cytometry of Annexin V/PI in NP cells treated with LPS. (F) Apoptotic cell rate of flow cytometry. Data are presented as the mean ± SD ($n = 3$, biological replicates).

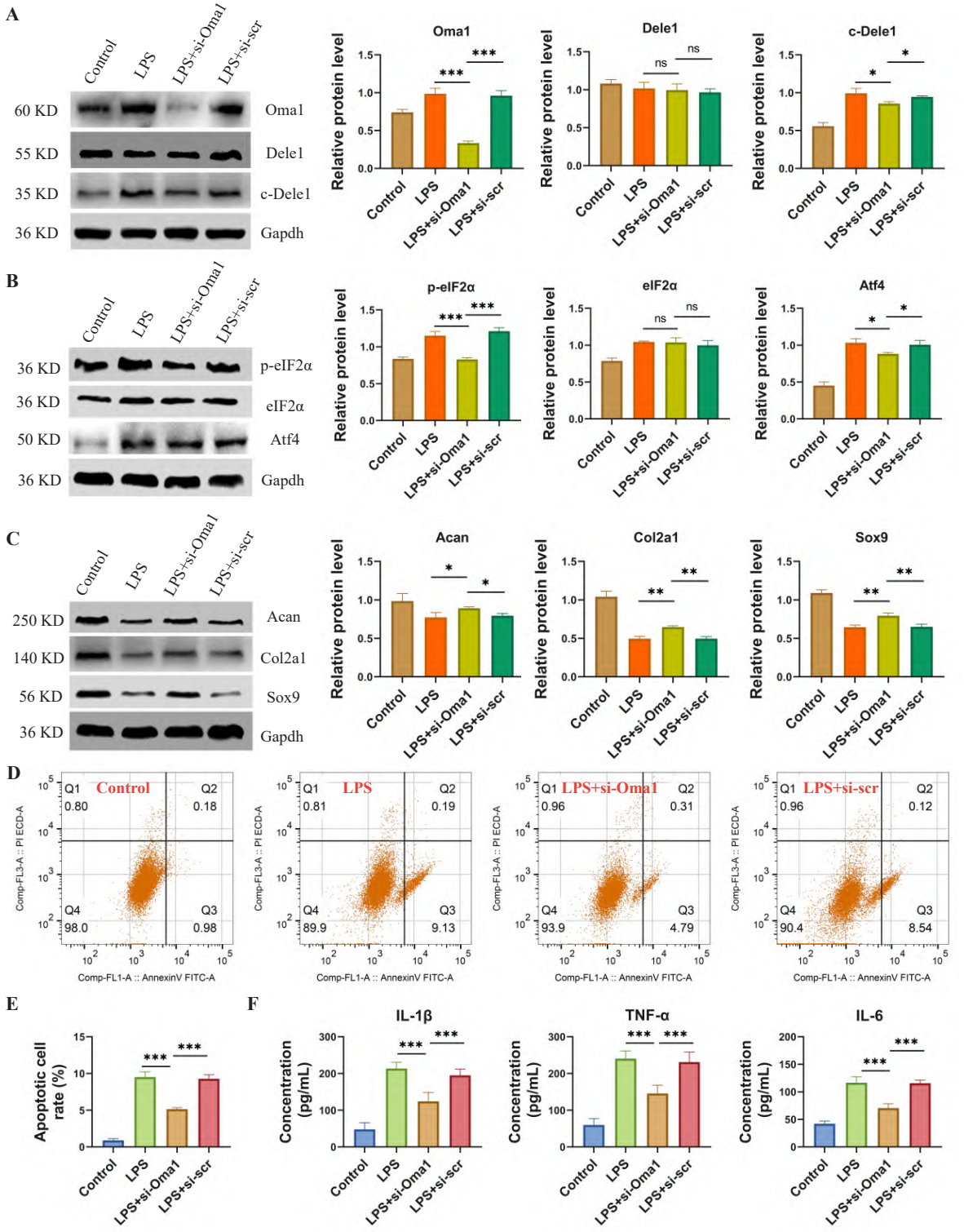

Fig. 2 OMA1 knockdown reduces the ISR in NP cells. (A) Western blot and quantitative analysis of OMA1, DELE1, and c-DELE1 in NP cells transfected with si-OMA1 or si-scr (50 nM). (B) Western blot and quantitative analysis of eIF2α, p-eIF2α, and ATF4 in NP cells transfected with si-OMA1 or si-scr. (C) Western blot and quantitative analysis of Acan, Col2a1, and Sox9 in NP cells transfected with si-OMA1 or si-scr. (D) Flow cytometry of Annexin V/PI in NP cells transfected with si-OMA1 or si-scr. (E) Apoptotic cell rate of flow cytometry. (F) ELISA results of secreted IL-1β, TNF-α, and IL-6 in NP cells transfected with si-OMA1 or si-scr. Data are presented as the mean ± SD ($n = 3$, biological replicates).

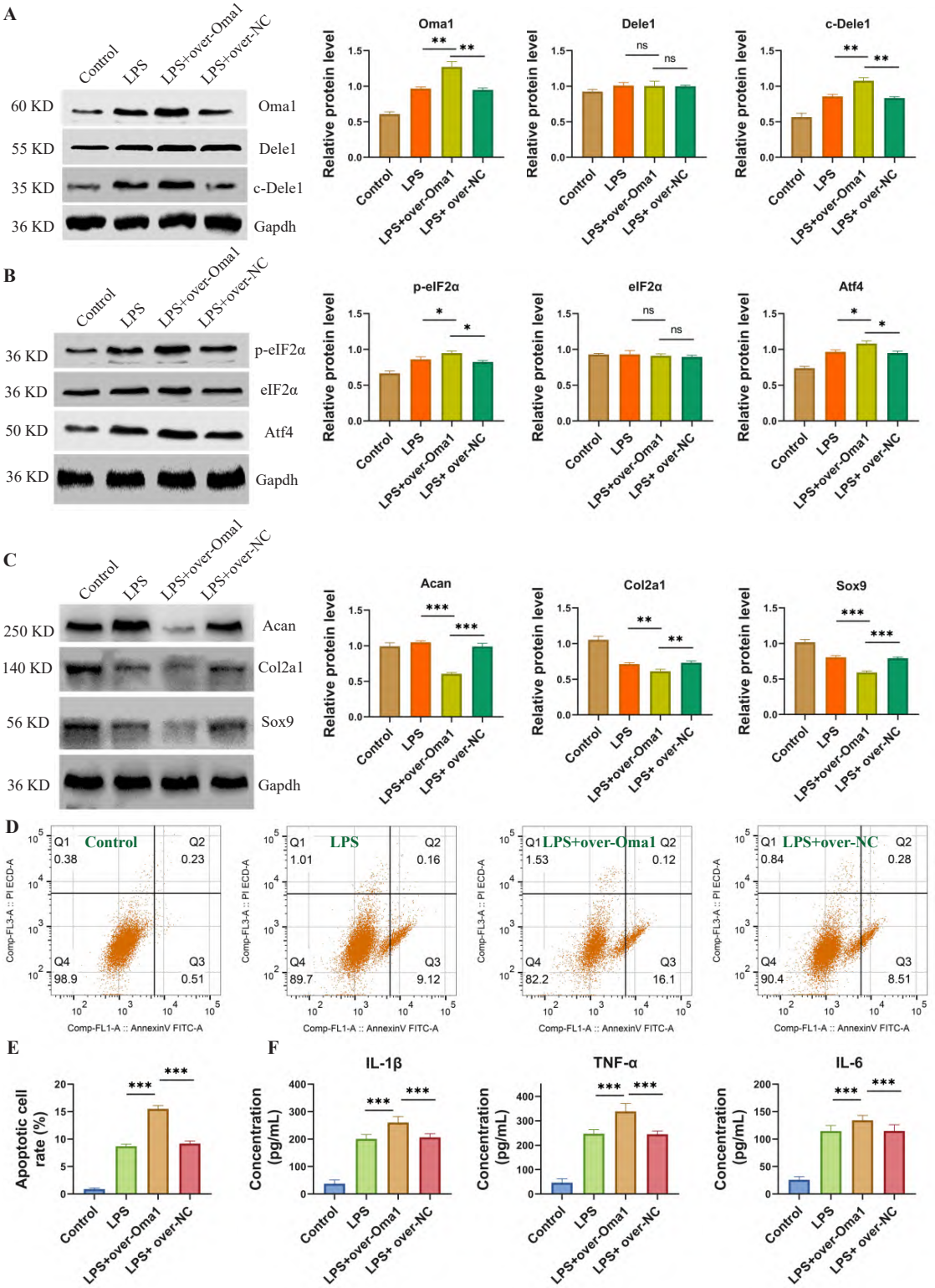

Fig. 3 OMA1 overexpression promotes the ISR in NP cells. (A) Western blot and quantitative analysis of OMA1, DELE1, and c-DELE1 in NP cells transfected with over-OMA1 or over-NC (2 μg/ml). (B) Western blot and quantitative analysis of eIF2α, p-eIF2α, and ATF4 in NP cells transfected with over-OMA1 or over-NC. (C) Western blot and quantitative analysis of Acan, Col2a1, and Sox9 in NP cells transfected with over-OMA1 or over-NC. (D) Flow cytometry of Annexin V/PI in NP cells transfected with over-OMA1 or over-NC. (E) Apoptotic cell rate of flow cytometry. (F) ELISA results of secreted IL-1β, TNF-α, and IL-6 in NP cells transfected with over-OMA1 or over-NC. Data are presented as the mean ± SD ($n = 3$, biological replicates).

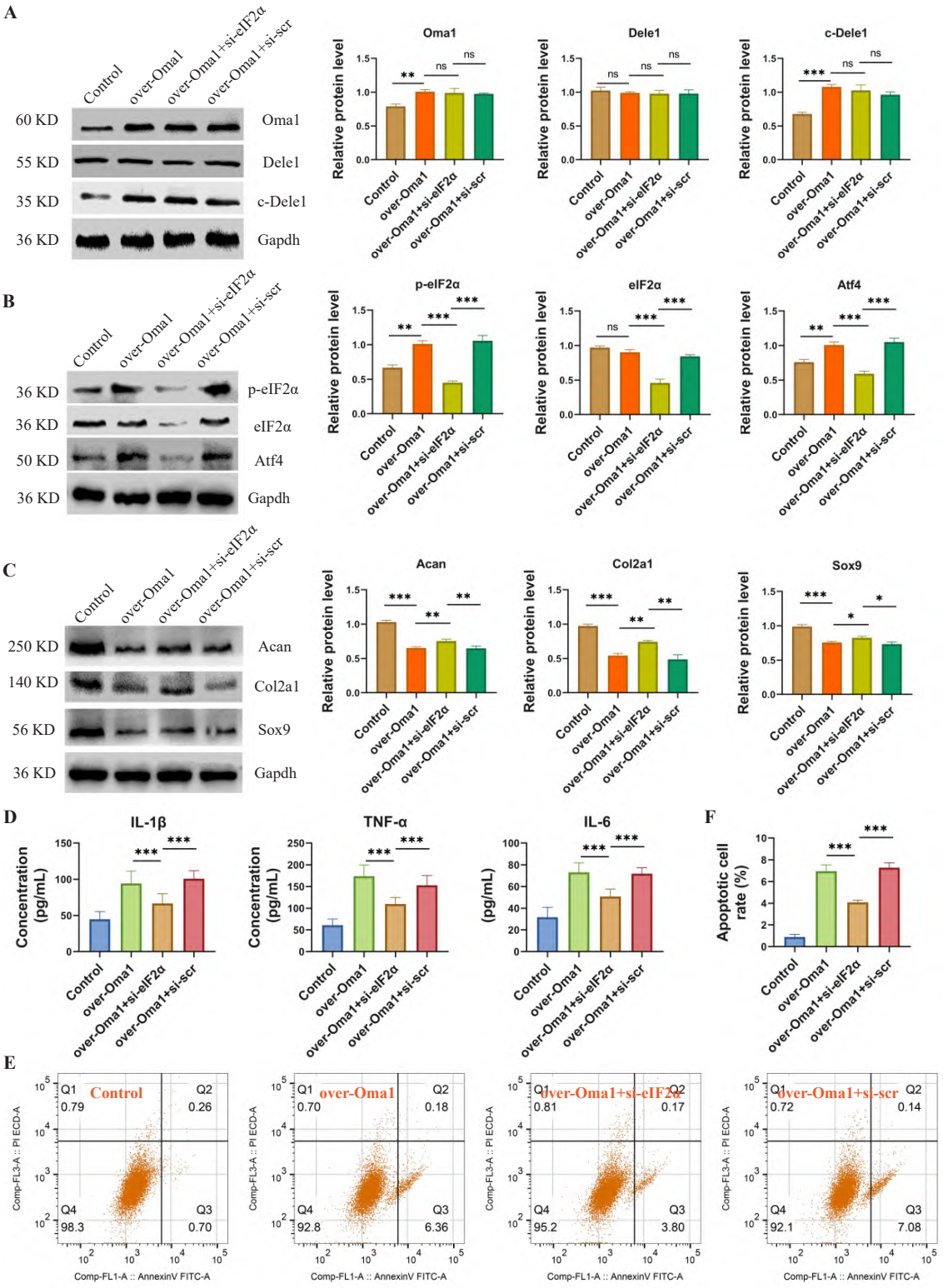

Fig. 4 OMA1 regulates the eIF2α/ATF4 signaling during the ISR. (A) Western blot and quantitative analysis of OMA1, DELE1, and c-DELE1 in NP cells transfected with over-OMA1 (2 μg/ml). and si-eIF2α (50 nM). (B) Western blot and quantitative analysis of eIF2α, p-eIF2α, and ATF4 in NP cells transfected with over-OMA1 and si-eIF2α. (C) Western blot and quantitative analysis of Acan, Col2a1, and Sox9 in NP cells transfected with over-OMA1 and si-eIF2α. (D) ELISA results of secreted IL-1β, TNF-α, and IL-6 in NP cells transfected with over-OMA1 and si-eIF2α. (E) Flow cytometry of Annexin V/PI in NP cells transfected with over-OMA1 and si-eIF2α. (F) Apoptotic cell rate of flow cytometry. Data are presented as the mean ± SD ($n = 3$, biological replicates).

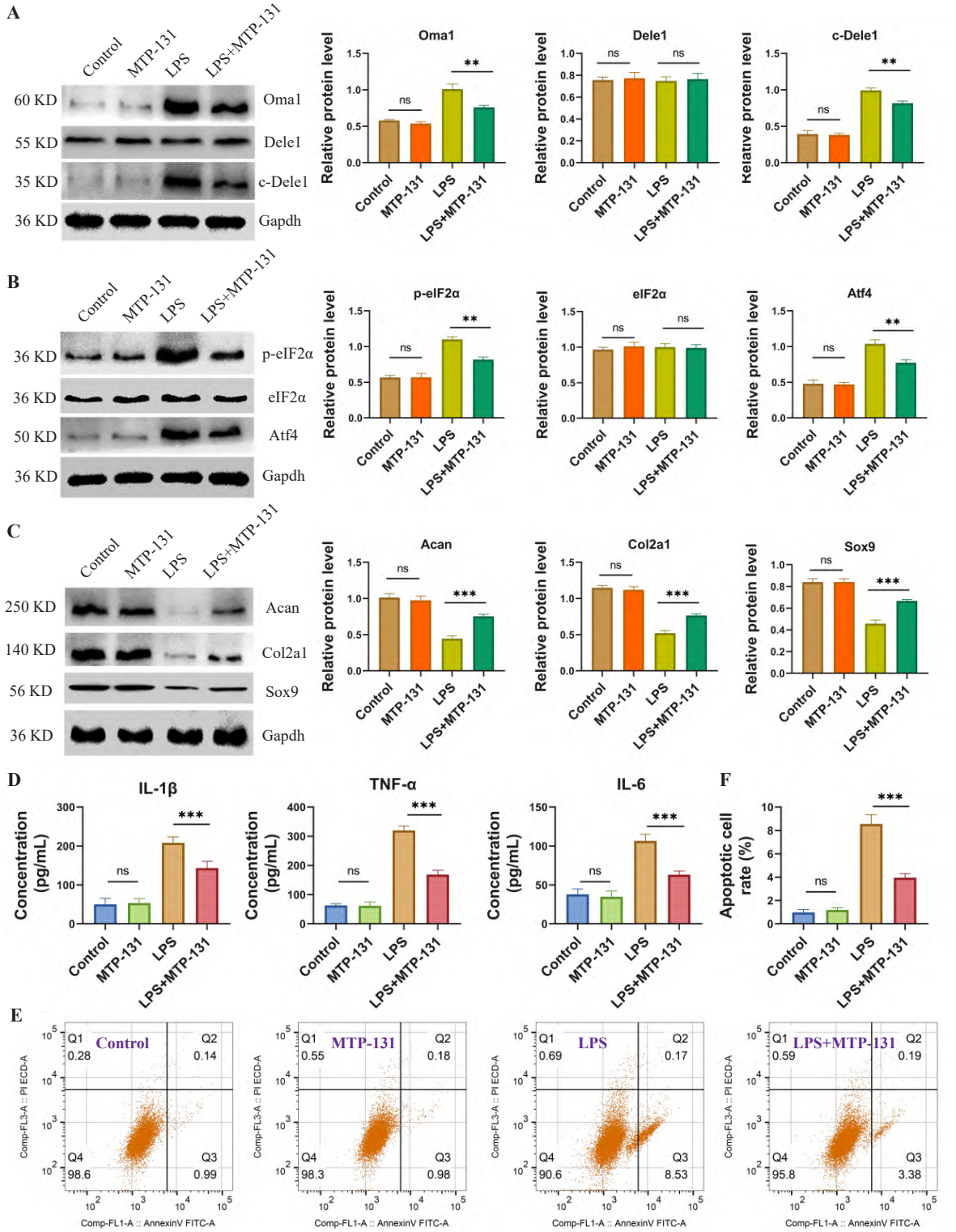

Fig. 5 MTP-131 coordinates the ISR in NP cells. (A) Western blot and quantitative analysis of OMA1, DELE1, and c-DELE1 in NP cells treated with LPS (1 μg/ml) and MTP-131 (1 μM). (B) Western blot and quantitative analysis of eIF2α, p-eIF2α, and ATF4 in NP cells treated with LPS and MTP-131. (C) Western blot and quantitative analysis of Acan, Col2a1, and Sox9 in NP cells treated with LPS and MTP-131. (D) ELISA results of secreted IL-1β, TNF-α, and IL-6 in NP cells treated with LPS and MTP-131. (E) Flow cytometry of Annexin V/PI in NP cells treated with LPS and MTP-131. (F) Apoptotic cell rate of flow cytometry. Data are presented as the mean ± SD ($n = 3$, biological replicates).

mediated apoptosis in NP cells (Fig. 5E,F). These data indicate that MTP-131 inhibits OMA1/DELE1 signaling and modulates ISR, thereby counteracting LPS-induced NP cell inflammation and apoptosis.

MTP-131 inhibits the OMA1 activation and affects the OMA1/DELE1 binding

To explore the mechanism by which MTP-131 regulates OMA1, we treated OMA1-overexpressed NP cells with MTP-131. OMA1 overexpression increased cytoplasmic c-DELE1 levels, while MTP-131 reduced its expression (Fig. 6A). Although OMA1 overexpression activated ISR, the treatment of MTP-131 significantly suppressed eIF2α phosphorylation and ATF4 expression (Fig. 6B). Co-immunoprecipitation assays revealed that MTP-131 had no significant effect on OMA1-DELE1 binding under normal conditions (Fig. 6C). However, under LPS-induced inflammatory conditions, MTP-131 inhibited OMA1-DELE1 interaction (Fig. 6D). Collectively, MTP-131 exerts protective effects on NP cells by modulating OMA1 activity to inhibit downstream ISR signaling.

DISCUSSION

This study supports the role of OMA1 in the integrated stress response and the potential of MTP-131 in mitigating NP cell degeneration (Fig. 7). Our findings demonstrate that silencing OMA1 expression alleviates LPS-induced inflammatory responses and ECM catabolism in NP cells under pathological conditions. Conversely, OMA1 overexpression exacerbates ISR activation, aggravating apoptosis, inflammation, and ECM degradation in NP cells. MTP-131 inhibits OMA1 activation and DELE1 cleavage, thereby attenuating ISR. Specifically, MTP-131 suppresses OMA1-DELE1 interaction under inflammatory conditions, reducing the generation and cytoplasmic translocation of DELE1 cleavage products. These findings may suggest MTP-131 as a promising mitochondria-targeted therapeutic agent with potential for IDD treatment.

Mitochondrial dysfunction is a key driver of IDD. Declines in mitochondrial membrane potential and impaired electron transport chain activity reduce ATP production efficiency, leading to metabolic disturbances and ROS accumulation, which exacerbate cellular damage [17]. Mitochondrial dysfunction often activates inflammatory pathways, promoting cytokine release, and accelerating ECM degradation [18]. For instance, mitochondrial DNA leakage activates the cGAS-STING pathway, amplifying immune responses and inducing cellular inflammation and senescence [19]. Zhang et al [20] discovered that oxidative stress can induce mitochondrial dysfunction, which is characterized by the opening of the mitochondrial permeability transition pore. This resulted in the release of mitochondrial DNA into the cytosol and, ultimately, the death of NP cells. Kang et al [21] discovered that mechanical stress promoted oxidative stress and mitochondrial dysfunction. This resulted in the accumulation of damaged mitochondria and impaired mitophagy, which in turn caused persistent oxidative damage to NP cells. In the present study, it was found that LPS induced mitochondrial stress, accompanied by the activation of OMA1 and the release of c-DELE1. The sustained activation of OMA1 has been demonstrated to promote the ISR activation, resulting in NP cell apoptosis.

The ISR is closely linked to organelle (e.g., mitochondrial, endoplasmic reticulum, and lysosome) damage [22, 23]. Mitochondrial and ER stress activate the ATF4/CHOP axis via eIF2α phosphorylation, triggering the unfolded protein response to mitigate stress [9]. Simultaneously, stress-induced activation of pro-apoptotic factors like BAX/BAK drives apoptosis [24]. While ISR initially promotes mitochondrial homeostasis, persistent stress disrupts cellular equilibrium, accelerating apoptosis [8, 25]. Xu et al [27] discovered that the expression of ATF4 and the integrated stress response pathway is elevated in mouse airways following influenza infection [26]. This elevation is associated with compromised mitochondrial function and cell apoptosis. Furthermore, the present study revealed that the ISR activated the eIF2α/ATF4 signaling and promoted cell apoptosis under the LPS treatment in NP cells. However, the potential dual role of ISR in the degeneration of NP cells remains to be elucidated through further investigation.

The phosphorylation of eIF2α serves as a convergence point for diverse stress signals [9]. The PRKR-like endoplasmic reticulum kinase, activated by mitochondrial damage, oxidative stress, or nutrient deprivation, phosphorylates eIF2α, driving ATF4 activation [28]. The eIF2α/ATF4 axis acts as a critical effector in ISR, balancing cellular adaptation and injury [29]. ATF4 regulates stress-adaptive gene transcription but may also exacerbate inflammatory damage. As demonstrated in the research, the activation of ATF4 has been shown to induce the ISR, thereby enhancing purine and pyrimidine biosynthesis [30]. Furthermore, it has been demonstrated that this process contributes to transcriptional and metabolic remodeling in renal cell carcinoma. In their study, Ahola et al [31] discovered that the deletion of ATF4 for the purpose of ISR inhibition resulted in impaired glutathione metabolism, particularly with regard to the activity of glutathione peroxidase (GPX4). This, in turn, led to an increase in lipid peroxidation, ultimately resulting in ferroptosis in cardiac cells. Similarly, the present study demonstrated that eIF2α knockdown significantly decreased the activation of eIF2α/ATF4 signaling and ISR, consequently inhibiting LPS-induced NP cell apoptosis.

OMA1, a mitochondrial inner membrane metalloprotease, plays a pivotal role in mitochondrial dynamics and ISR [32]. Activated OMA1 cleaves OPA1 to regulate mitochondrial fusion and processes DELE1

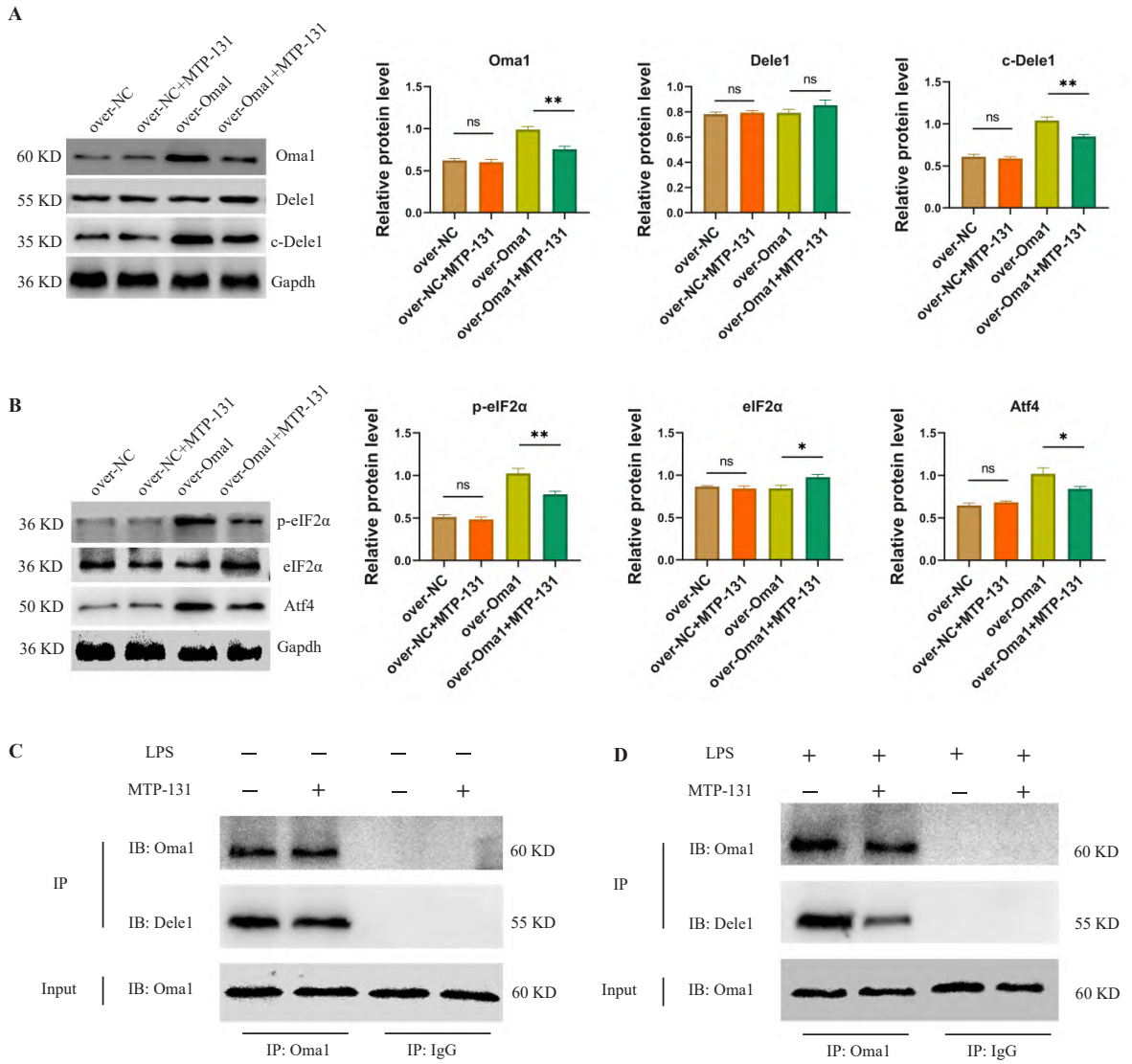

Fig. 6 MTP-131 affects the OMA1/DELE1 binding during the ISR. (A) Western blot and quantitative analysis of OMA1, DELE1, and c-DELE1 in NP cells treated with over-OMA1 and MTP-131. (B) Western blot and quantitative analysis of eIF2α, p-eIF2α, and ATF4 in NP cells treated with over-OMA1 and MTP-131. (C) co-IP results of OMA1 and DELE1 in normal NP cells treated with or without MTP-131. (D) co-IP results of OMA1 and DELE1 in LPS-treated NP cells treated with or without MTP-131. IgG serves as a negative control. Data are presented as the mean ± SD ($n = 3$, biological replicates).

to promote eIF2α phosphorylation and HRI kinase activation, thereby modulating ISR [31]. Beyond mitochondrial dynamics, OMA1 determines cell fate via protease-dependent signaling pathways [33]. Shammas et al [34] discovered that OMA1 is associated with the mitochondrial fragmentation, and that it delivers a signal outside the mitochondria to activate the integrated stress response through the cleavage of DELE1. A further study has indicated that the OMA1-OPA1 axis is activated under conditions of hypoxia, thereby increasing mitochondrial ROS accumulation and thereby inhibiting mitochondrial oxidative phosphorylation [35]. This, in turn, promotes glycolysis and metabolic reprogramming in cancer cells. The results of the present study demonstrate that OMA1 induces the cleavage of DELE1, thereby activating the ISR and promoting NP cell degeneration.

The mitochondria-targeted peptide MTP-131 enhances mitochondrial function by stabilizing electron transport chains via cardiolipin binding, thereby improving ATP synthesis and suppressing ROS [15]. It stabilizes mitochondrial membrane potential, mitigates mitochondrial damage, and inhibits apoptosis [13]. Additionally, MTP-131 promotes Parkin/PINK1-dependent mitophagy, maintaining mitochondrial quality control [36]. It has been demonstrated that

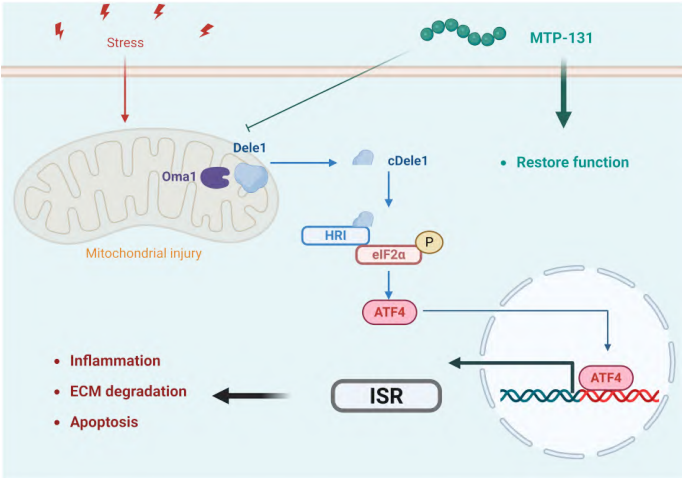

Fig. 7 The schematic diagram depicts the OMA1/DELE1-mediated activation of the ISR in NP cells. MTP-131 regulates the OMA1/DELE1 binding and restore cell function to protect against NP cell degeneration.

MTP-131 activates the PINK1-mediated process of mitophagy, thereby mitigating oxidative stress and restoring mitochondrial function in oral epithelial cells [37]. The protective properties of MTP-131 suggest its potential application in the treatment of neurodegenerative diseases, cardiovascular ischemia-reperfusion injury, and chronic inflammatory disorders. Furthermore, our results demonstrated that MTP-131 suppresses OMA1-DELE1 interaction under inflammatory conditions, thereby reducing the generation and cytoplasmic translocation of DELE1 cleavage. Treatment with MTP-131 could inhibit the OMA1 activation and DELE1 cleavage. This, in turn, has been shown to attenuate ISR and ameliorate NP cell degeneration. The present findings suggest that MTP-131 may be a promising candidate for IDD treatment.

While this study provides novel insights into the OMA1-ISR axis in IDD, several limitations must be acknowledged. First, the use of LPS-induced inflammation *in vitro* does not fully replicate the complex microenvironment of human degenerative discs. Second, OMA1's broader roles in mitochondrial dynamics, mitochondrial ROS production, ATP levels, or mitochondrial morphology were not explored. Third, the reliance on genetic modulation may introduce off-target effects, necessitating validation using tissue-specific conditional knockout models. Finally, the addition of cytosolic and mitochondrial fractionation experiments would provide more rigorous scientific validation of the relationship between OMA1 activity, ISR signaling activation, and mitochondrial function.

This study suggests a previously unrecognized pathway that may link mitochondrial dysfunction to ISR activation in IDD. Our findings indicate that OMA1-mediated DELE1 cleavage may serve as a mitochondrial stress sensor, potentially triggering eIF2α phosphorylation and downstream ISR signaling. The therapeutic efficacy of MTP-131 observed in this study supports a possible role in stabilizing mitochondrial membranes and suppressing ISR hyperactivation. Notably, its regulation of OMA1-DELE1 binding under inflammatory conditions may help address a key mechanistic gap in ISR regulation. These findings are in line with prior work on mitochondrial-targeted therapies in IDD, and they suggest the therapeutic potential of MTP-131 for disc degeneration.

REFERENCES

1. Wang Y, Cheng H, Wang T, Zhang K, Zhang Y, Kang X (2023) Oxidative stress in intervertebral disc degeneration: Molecular mechanisms, pathogenesis and treatment. *Cell Prolif* **56**, e13448.
2. Liao Zw, Ke Wc, Liu H, Tong B, Wang K, Feng Xb, Hua Wb, Wang Bg, et al (2022) Vasorin-containing small extracellular vesicles retard intervertebral disc degeneration utilizing an injectable thermoresponsive delivery system. *J Nanobiotechnology* **20**, 420.
3. Zhang G-Z, Deng Y-J, Xie Q-Q, Ren E-H, Ma Z-J, He X-G, Gao Y-C, Kang X-W (2020) Sirtuins and intervertebral disc degeneration: Roles in inflammation, oxidative stress, and mitochondrial function. *Clin Chim Acta* **508**, 33–42.
4. Tu H, Gao Q, Zhou Ym, Peng L, Wu D, Zhang Dm, Yang J (2024) The role of sirtuins in intervertebral disc degeneration: Mechanisms and therapeutic potential. *J Cell Physiol* **239**, e31328.
5. Liao Zw, Zhu Dc, Ou Zx, Zhao Mk, Zhao Kc, Tong B, Yang C, Li S (2026) TDP43 cytoplasmic mislocalization initiates mitochondrial dysfunction and intercellular senescence propagation in intervertebral disc degeneration. *Exp Mol Med* **58**, 1464–1478.
6. Liao Zw, Tong B, Ke Wc, Yang C, Wu Xh, Lei M (2024) Extracellular vesicles as carriers for mitochondria: Biological functions and clinical applications. *Mitochondrion* **78**, 101935.
7. Ou Zx, Wei Jy, Tong B, Lei J, Liang Hz, Zhu Dc, Wang Hc, Zhou Xy, et al (2025) Taurine can restrict MtdsRNA

mediated pyroptosis by enhancing mitophagy in nucleus pulposus cells. *Cell Commun Signal* **23**, 423.

8. Lu H-J, Koju N, Sheng R (2024) Mammalian integrated stress responses in stressed organelles and their functions. *Acta Pharmacol Sin* **45**, 1095–1114.
9. Donnelly N, Gorman AM, Gupta S, Samali A (2013) The eIF2α kinases: Their structures and functions. *Cell Mol Life Sci* **70**, 3493–3511.
10. Liao Zw, Liu H, Ma L, Lei J, Tong B, Li Gc, Ke Wc, Wang K, et al (2021) Engineering extracellular vesicles restore the impaired cellular uptake and attenuate intervertebral disc degeneration. *ACS Nano* **15**, 14709–14724.
11. Yamada T, Ikeda A, Murata D, Wang H, Zhang C, Khare P, Adachi Y, Ito F, et al (2025) Dual regulation of mitochondrial fusion by Parkin-PINK1 and OMA1. *Nature* **639**, 776–783.
12. Guo Xy, Aviles G, Liu Y, Tian R, Unger BA, Lin YT, Wiita AP, Xu K, et al (2020) Mitochondrial stress is relayed to the cytosol by an OMA1-DELE1-HRI pathway. *Nature* **579**, 427–432.
13. Tung C, Varzideh F, Farroni E, Mone P, Kansakar U, Jankauskas SS, Santulli G (2025) Elamipretide: A review of its structure, mechanism of action, and therapeutic potential. *Int J Mol Sci* **26**, 944.
14. Nhu NT, Xiao S-Y, Liu Yj, Kumar VB, Cui Z-Y, Lee S-D (2022) Neuroprotective effects of a small mitochondrially-targeted tetrapeptide elamipretide in neurodegeneration. *Front Integr Neurosci* **15**, 747901.
15. Obi C, Smith AT, Hughes GJ, Adeboye AA (2022) Targeting mitochondrial dysfunction with elamipretide. *Heart Fail Rev* **27**, 1925–1932.
16. Sabbah HN, Alder NN, Sparagna GC, Bruce JE, Stauffer BL, Chao LH, Pitceathly RDS, Maack C, et al (2025) Contemporary insights into elamipretide's mitochondrial mechanism of action and therapeutic effects. *Biomed Pharmacother* **187**, 118056.
17. Zorov DB, Juhaszova M, Sollott SJ (2014) Mitochondrial reactive oxygen species (ROS) and ROS-induced ROS release. *Physiol Rev* **94**, 909–950.
18. Youle RJ, Van Der Bliek AM (2012) Mitochondrial fission, fusion, and stress. *Science* **337**, 1062–1065.
19. Yan Cj, Duanmu Xy, Zeng L, Liu B, Song Zy (2019) Mitochondrial DNA: Distribution, mutations, and elimination. *Cells* **8**, 379.
20. Zhang Wf, Li Gc, Luo Rj, Lei J, Song Y, Wang Bj, Ma L, Liao Zw, et al (2022) Cytosolic escape of mitochondrial DNA triggers cGAS-STING-NLRP3 axis-dependent nucleus pulposus cell pyroptosis. *Exp Mol Med* **54**, 129–142.
21. Kang L, Liu Sw, Li Jc, Tian Yy, Xue Y, Liu Xz (2020) The mitochondria-targeted anti-oxidant MitoQ protects against intervertebral disc degeneration by ameliorating mitochondrial dysfunction and redox imbalance. *Cell Prolif* **53**, e12779.
22. Tian Xb, Zhang Sl, Zhou Ll, Seyhan AA, Borrero LH, Zhang Yq, El-Deiry WS (2021) Targeting the integrated stress response in cancer therapy. *Front Pharmacol* **12**, 747837.
23. Liao Zw, Ou Zx, Tong B, Li S, Yang C (2025) Customized extracellular vesicles targeting lysosomal biogenesis deliver therapeutic cargo for intervertebral disc degeneration treatment. *J Nanobiotechnology* **23**, 659.
24. Winter JM, Yadav T, Rutter J (2022) Stressed to death: Mitochondrial stress responses connect respiration and apoptosis in cancer. *Mol Cell* **82**, 3321–3332.
25. Pakos-Zebrucka K, Koryga I, Mnich K, Ljujic M, Samali A, Gorman AM (2016) The integrated stress response. *EMBO Rep* **17**, 1374–1395.
26. Xu L, Tan Ct, Barr J, Talaba N, Verheyden J, Chin JS, Gaboyan A, Kasaraneni N, et al (2024) Context-dependent roles of mitochondrial LONP1 in orchestrating the balance between airway progenitor versus progeny cells. *Cell Stem Cell* **31**, 1465–1483.
27. Liao Zw, Tong B, Zhang Xg, Zhang Wf, Ke Wc, Liang Hz, Lei M, Hua Wb, et al (2023) Selective cargo sorting in stem cell-derived small extracellular vesicles: Impact on therapeutic efficacy for intervertebral disc degeneration. *Clin Transl Med* **13**, e1494.
28. Balsa E, Soustek MS, Thomas A, Cogliati A, García-Poyatos C, Martín-García E, Jedrychowski M, Gygi SP, et al (2019) ER and nutrient stress promote assembly of respiratory chain supercomplexes through the PERK-eIF2α axis. *Mol Cell* **74**, 877–890.
29. Tang H, Kang R, Liu J, Tang Dl (2024) ATF4 in cellular stress, ferroptosis, and cancer. *Arch Toxicol* **98**, 1025–1041.
30. Van Der Mijn JC, Chen Qy, Laursen KB, Khani F, Wang Xf, Dorsaint P, Sboner A, Gross SS, et al (2022) Transcriptional and metabolic remodeling in clear cell renal cell carcinoma caused by ATF4 activation and the integrated stress response (ISR). *Mol Carcinog* **61**, 851–864.
31. Ahola S, Mejías PR, Hermans S, Chandragiri S, Giavalisco P, Nolte H, Langer T (2022) OMA1-mediated integrated stress response protects against ferroptosis in mitochondrial cardiomyopathy. *Cell Metab* **34**, 1875–1891.
32. Alavi MV (2022) Recent advances in, and challenges of, designing OMA1 drug screens. *Pharmacol Res* **176**, 106063.
33. Alavi MV (2020) OMA1: An integral membrane protease? *Biochim Biophys Acta Proteins Proteom* **1869**, 140558.
34. Shammas MK, Huang Xp, Wu BP, Fessler E, Song IY, Randolph NP, Li Y, Bleck CK, et al (2022) OMA1 mediates local and global stress responses against protein misfolding in CHCHD10 mitochondrial myopathy. *J Clin Invest* **132**, e157504.
35. Wu Zd, Zuo Ml, Zeng L, Cui Ks, Liu B, Yan Cj, Chen L, Dong J, et al (2020) OMA1 reprograms metabolism under hypoxia to promote colorectal cancer development. *EMBO Rep* **22**, e50827.
36. Liao Zw, Li Sa, Lu Sd, Liu H, Li Gc, Ma L, Luo Rj, Ke Wc, et al (2021) Metformin facilitates mesenchymal stem cell-derived extracellular nanovesicles release and optimizes therapeutic efficacy in intervertebral disc degeneration. *Biomaterials* **274**, 120850.
37. Ye P, Liu H, Qin Y, Li Z, Huang Z, Bu X, Peng Q, Duan N, et al (2024) SS-31 mitigates oxidative stress and restores mitochondrial function in cigarette smoke-damaged oral epithelial cells via PINK1-mediated mitophagy. *Chem Biol Interact* **400**, 111166.